Electronic Supplementary Material (ESI) for Analytical Methods

Supporting Information

A redox modulated fluorescence nanoplatform for detection of alkaline phosphatase activity with fluorescent polydopamine nanoparticles

Jing-Xuan Tian[1], Yan-Zhao Fang[1], Rui Yu[1], Zi-Yan Zhang[1], Yan-Tong Zhuo[1], Jia-Yu He[1], Shuang Wu[2], Qiang Xiao*[1] and Xiang-Juan Kong*[1]

*1 Jiangxi Key Laboratory of Organic Chemistry, Jiangxi Science and Technology Normal University, Nanchang 330013, P. R. China**

2 A Key Laboratory of Jiangxi Province for Persistent Pollutants Control and Resources Recycle, Nanchang Hangkong University, Nanchang 330063, P. R. *China.*

Email: xiaoqiang@tsinghua.org.cn; xiangjuankong@163.com

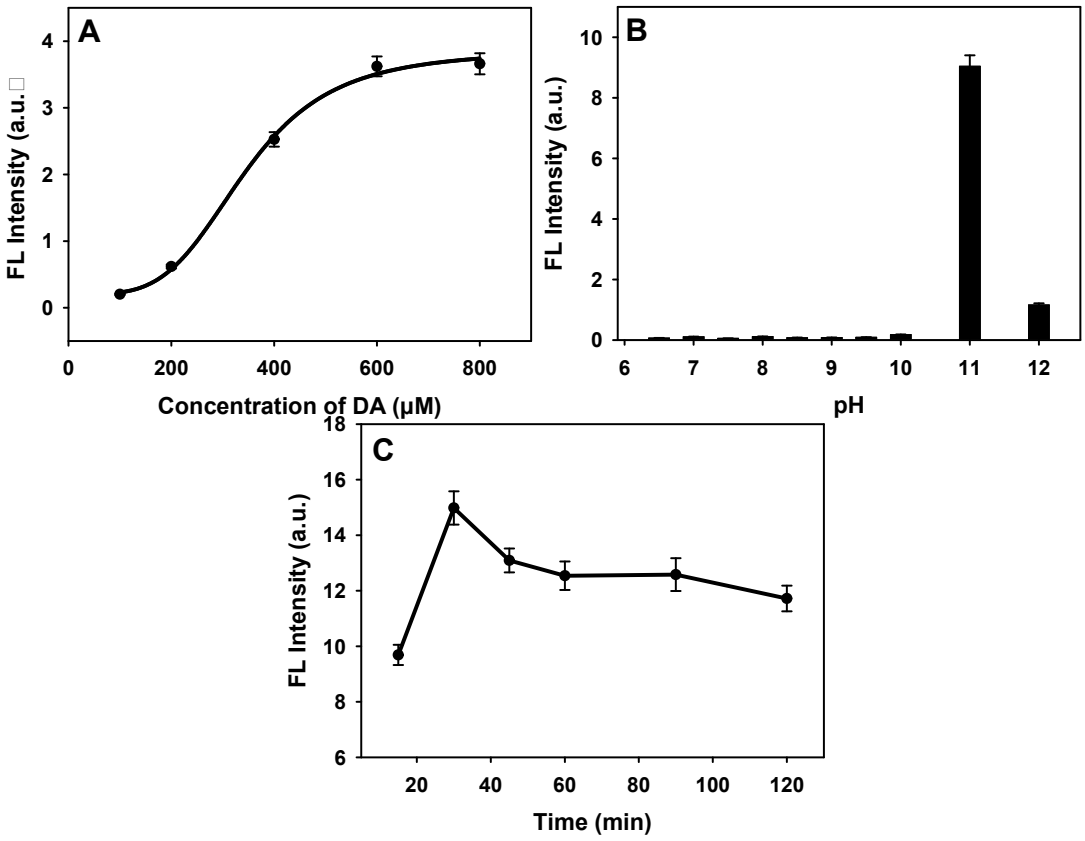

Fig. S1 Optimization of the reaction conditions for fluorescent PDA NPs synthesis. (A) The effect of the DA concentration on the fluorescence intensity of PDA NPs. (B) The effect of the solution pH on the fluorescence intensity of PDA NPs. (C) Variance of the fluorescence intensity with reaction time of DA oxidization and autopolymerization. Error bars represent the standard deviation of three experiments.

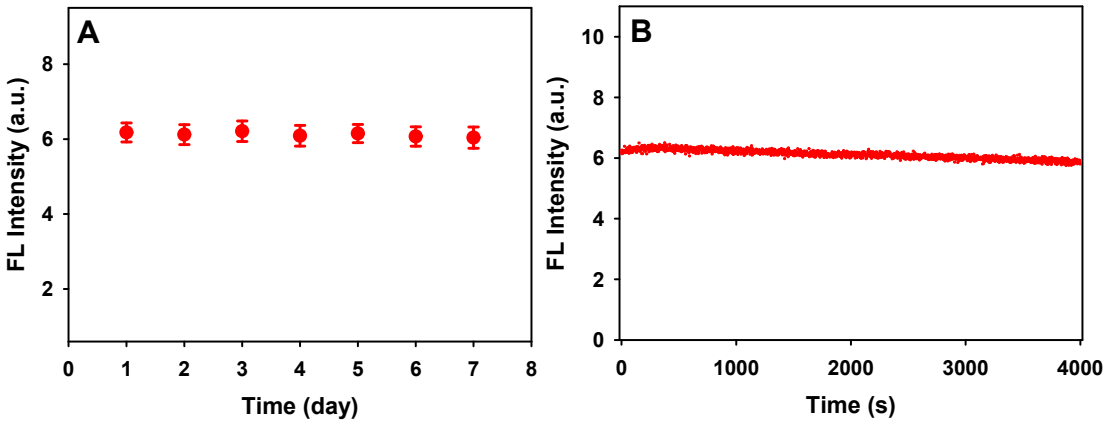

Fig. S2 The photostability of the formed PDA NPs in solutions (A) within different days (50 μL 2 mM PB solution, pH 7.0 +10 μL fluorescent PDA NPs +40 μL sterilized water) and (B) under continuous irradiation with 418nm excitation light (50 μL 2 mM PB solution, pH 7.0 +10 μL fluorescent PDA NPs +40 μL sterilized water). Error bars represent standard deviation of three repetitive experiments.

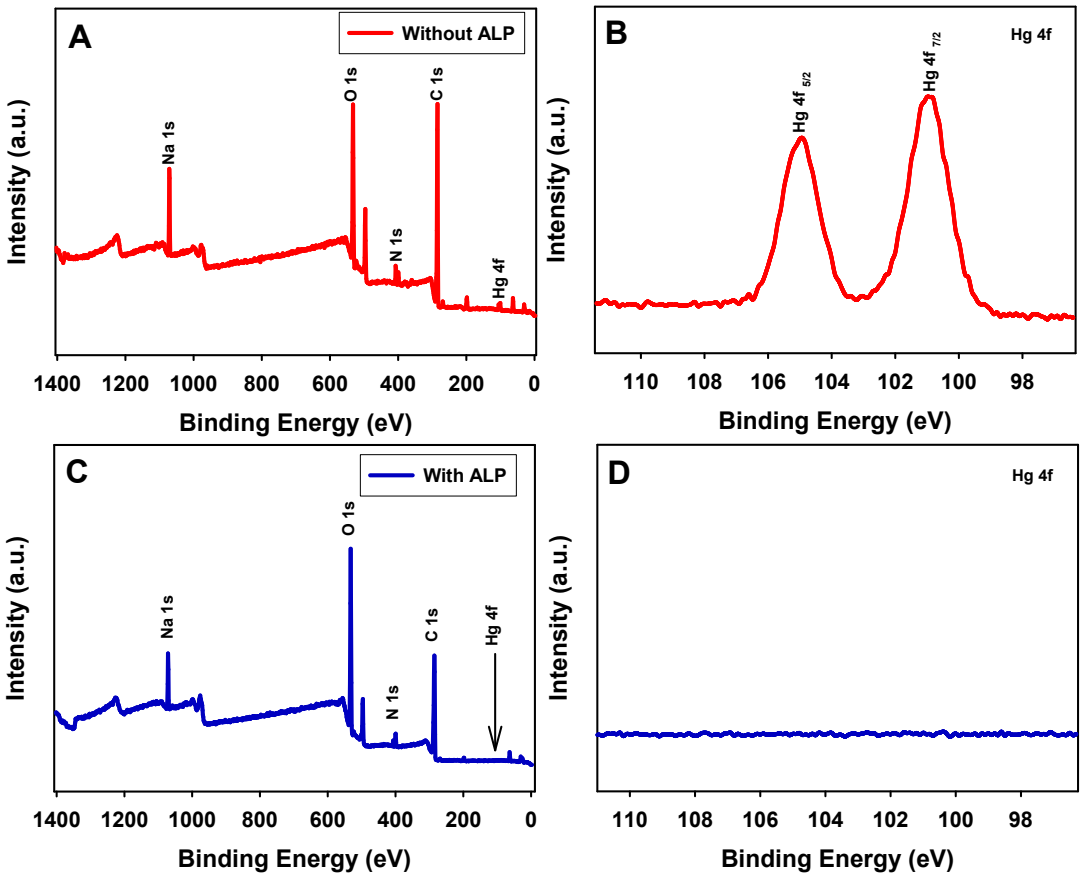

Fig. S3 XPS analysis and high-resolution of XPS spectra of Hg^{2+} on the surface of PDA NPs with ALP (A and B) and without ALP (C and D).

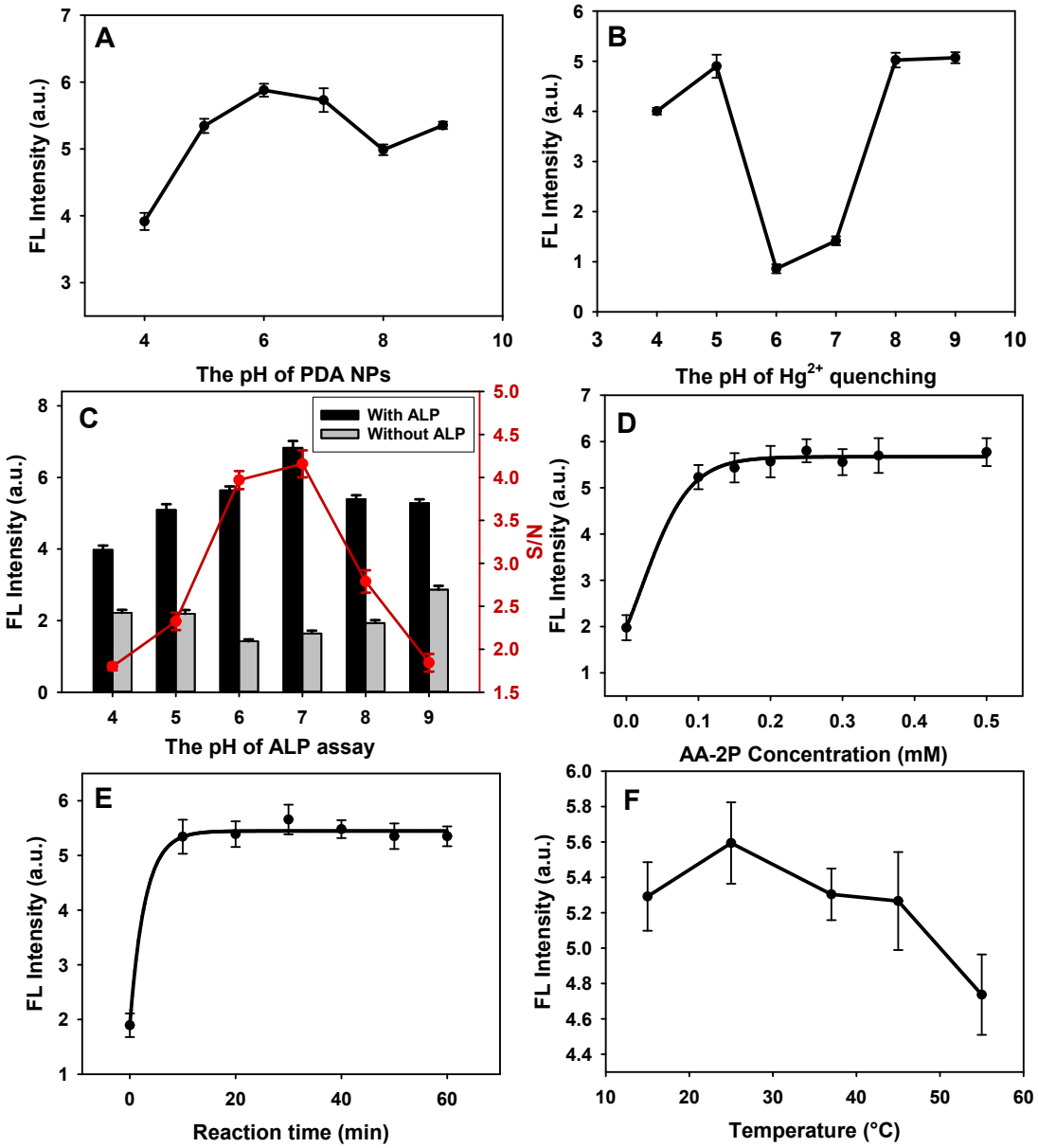

Fig. S4 Optimization of the experimental conditions for ALP detection. (A) The effect of the solution pH on the fluorescence intensity of PDA NPs. (B) The effect of the solution pH on the coordination reaction between Hg^{2+} and PDA NPs. (C) The effect of the solution pH on the enzymatic hydrolysis of ALP to AA2P. (D) Variance of the fluorescence intensity with the concentration of AA2P for ALP activity detection. (E) Variance of the fluorescence intensity with reaction time for ALP detection. (F) Variance of the fluorescence intensity with reaction temperature ALP detection. Error bars represent the standard deviation of three experiments. The conditions of pH 7.0, AA2P 0.15 mM, reaction time of 20 min and reaction temperature of 25°C were selected for ALP activity detection.

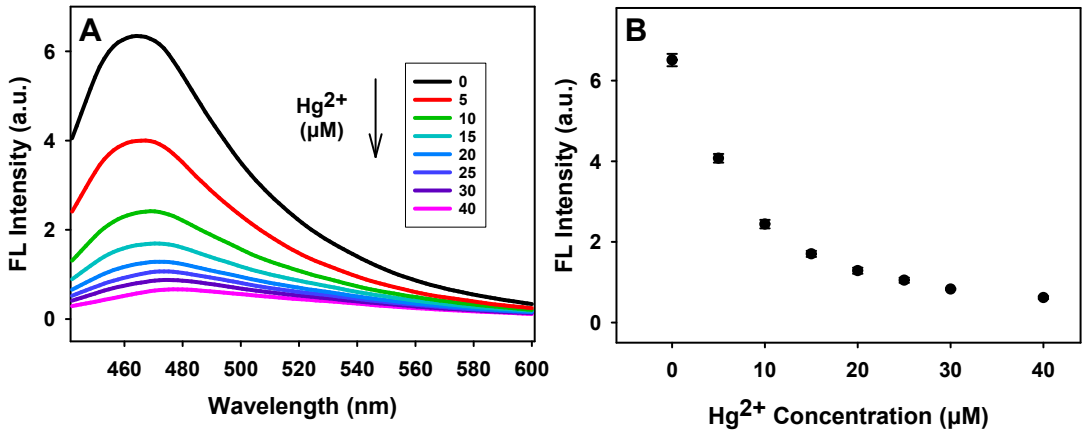

Fig. S5 (A) Fluorescence spectra of PDA NPs after incubation with various concentrations of Hg^{2+}. (B) Plot of fluorescence quenching responces versus Hg^{2+} concentration. Error bars represent the standard deviation of three experiments. 20 μM of Hg^{2+} was selected for ALP activity detection.

Table S1. Comparison the sensitivity of the reported analytical methods for ALP detection with our strategy

Method	Nanomaterials preparation time	Detection time (min)	Detection Limit (U/L)	Strategy	Ref.
Colorimetry	Over night	60	3.3	A high-resolution colorimetric method based on gold/silver core/shell nanorod for visual readout of ALP activity by using bare-eyes	1
Fluorescence	65 min	130	5	Copper-mediated on–off switch for detecting either pyrophosphate or ALP based on DNA-scaffolded silver nanoclusters	2
Colorimetry	--	75	5.4	Naked-eye sensitive detection of ALP and pyrophosphate based on a horseradish peroxidase catalytic colorimetric system with Cu (II)	3
Fluorescence and Colorimetry	1 h	45	0.2 and 0.5	Self-assembled gold nanoclusters for fluorescence turn-on and colorimetric dual-readout detection of alkaline phosphatase activity	4
Colorimetry	--	35	2.3	Colorimetric detection of ALP activity based on phosphate anion-quenched oxidase-mimicking activity of Ce(Ⅳ) ions	5
Fluorescence	12 h	55	1.48	A redox modulated ratiometric fluorometric method based on the use of dual-color carbon dots for determination of the activity of enzymes participating in ascorbic acid-related reactions	6
Fluorescence	2 days	35	0.1	Determination of the activity of alkaline phosphatase by using nanoclusters composed of flower-like cobalt oxyhydroxide and copper nanoclusters as fluorescent probes	7
Fluorescence	60 min	30	0.4	Fluorescent PDA NPs serving as signal indicator based on Hg^{2+}-induced fluorescence quenching and AA-triggered fluorescence recovery	This work

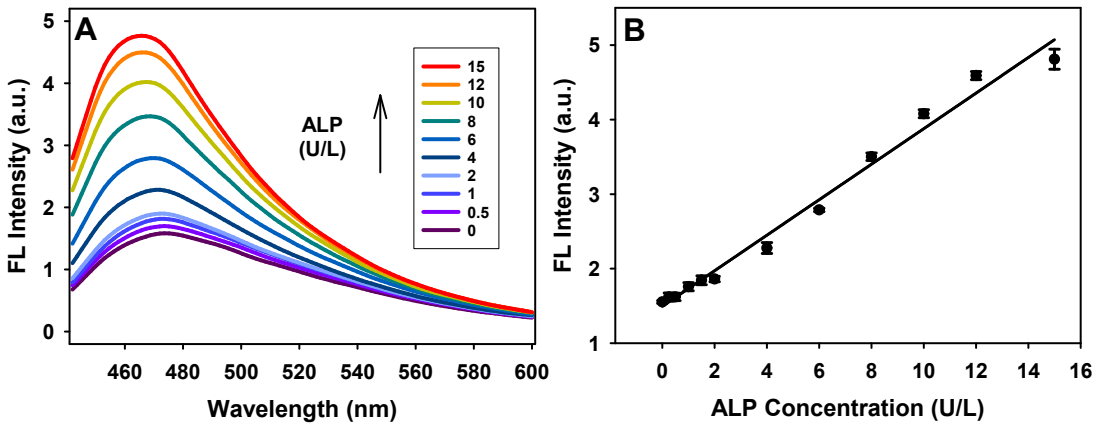

Fig. S6 Calibration curve of the nanoplatform for ALP detection in diluted serum samples. (A) Fluorescence responses of the PDA NPs as a function of ALP (0-15 U/L) in human serum. (B) Plot of the fluorescence intensity values against ALP concentration. The difference of the linear responses in Tris buffer and in diluted serum samples might be ascribed to the coordinate effect of Hg^{2+} with the proteins existing in serum samples, which interfered the redox reaction between Hg^{2+} and the product AA. Error bars represent the standard deviation of three experiments.

Table S2. Recovery detection of ALP in 0.5% human serum samples

	Added (U/L)	Found (U/L)	recovery	RSD (n=3)
1	2	1.92	96.0%	3.7%
2	6	5.87	97.8	5.4%
3	10	10.33	103.3%	5.3%
4	15	14.89	99.3%	5.0%

References:

1. Z. Q. Gao, K. C. Deng, X. D. Wang, M. Miro and D. P. Tang, *ACS Appl. Mater. Interfaces*, 2014, **6**, 18243-18250.

2. J. L. Ma, B. C. Yin, X. Wu and B. C. Ye, *Anal. Chem.,* 2016, **88**, 9219-9225.

3. D. M. Shi, Y. Sun, L. Lin, C. J. Shi, G. F. Wang and X. J. Zhang, *Analyst*, 2016, **141**, 5549-5554.

4. X. Han, M. Han, L. Ma, F. Qu, R. M. Kong and F. Qu, *Talanta,* 2019, 194, 55-62.

5. H. W. Song, H. Y. Wang, X. Li, Y. X. Peng, J. M. Pan and X. H. Niu, *Anal. Chim. Acta*, 2018, **1044**, 154-161.

6. X. Cheng, J. Xu, L. Wang, G. Xu, F. Wei, Y. Chai, H. Qin and Y. Cen, *Microchim. Acta,* 2019, **186**, 818.

7. H. B. Wang, Y Li, Y. Chen, Z. P. Zhang, T. Gan and Y. M. Liu, *Microchim. Acta*, 2018, **185**: 102.